Selective Adhesion of Hepatocytes on Patterned Surfaces[a]

S. N. BHATIA,[b,d] M. TONER,[b,e] R. G. TOMPKINS,[b]
AND M. L. YARMUSH[b,c]

[b]*Surgical Services*
Massachusetts General Hospital
Shriners Burns Institute
and
Department of Surgery
Harvard Medical School
Boston, Massachusetts 02114

[c]*Department of Chemical and Biochemical Engineering*
Rutgers University
Piscataway, New Jersey 08855

INTRODUCTION

Liver failure is the cause of death for approximately 30,000 patients in the United States annually. Given the scarcity of donor organs, alternative short- and long-term therapeutic solutions are needed. For temporary support, an extracorporeal bioartificial liver device would be ideal. However, in order for this dream to become a reality, designs and techniques for (1) maintaining hepatocytes in a stable, differentiated state, (2) efficient mass transport, and (3) placing a large number of cells in a small volume are needed.

Conventional approaches to bioartificial liver support include cultured monolayers,[1,2] hollow fibers,[2–8] microcarriers,[9,10] and combinations thereof.[11,12] Although these approaches have been partially successful in a number of *in vitro* and *in vivo* models, there are at least two major interactive areas where improvements would be beneficial: hepatocyte functional stability, and overall volume reduction and efficient mass transport to the cells. Stable cell masses would maximize efficient usage of the cell source and allow prolonged patient treatment. Small volumes of perfused fluid would minimize priming of the extracorporeal circuit and necessitate smaller numbers of cells to maintain physiologic concentrations of plasma factors. It has been recently shown that a sandwich culture configuration, which mimics the *in vivo* environment of hepatocytes, produces stable, differentiated cultures for up to 6 weeks.[13,14] One approach to a bioartificial liver, depicted in FIGURE 1, would involve the use of micropatterning technology to create rows of sandwiched hepatocytes that

[a]This work was supported by Grants from Shriner's Hospital for Crippled Children, NIH (DK-43371 and DK-41709), and the Office of Naval Research Graduate Fellowship Program.

[d]S. N. Bhatia is a graduate student in the Department of Mechanical Engineering, Massachusetts Institute of Technology, Cambridge, MA 02139.

[e]Address correspondence to Mehmet Toner, Ph.D., Shriners Burns Institute Research Center, One Kendall Square, Bldg. 1400W, Cambridge, MA 02139.

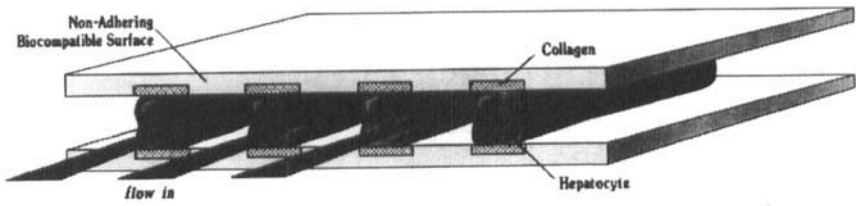

FIGURE 1. Schematic of a hypothetical micropatterned device: microchannel bioreactor.

would alternate with hepatocyte-free regions for the perfusion of fluid and efficient transport.

Micropatterning using photolithographical techniques has been used by others to obtain ordered arrays of various cell types on photochemically modified substrates[15–17] with pattern resolution on the order of 20 to 150 μm. This pattern resolution is adequate for hepatocytes; however, photolithographic techniques typically require the use of a limited class of coatings. Because hepatocytes have been shown to function well when cultured on collagen-based coatings,[18] one plausible approach to obtaining hepatocellular patterning is to first obtain a collagen pattern on a solid substrate. Selective deposition of collagen could be achieved by creating a hydrophobic and hydrophilic polymer pattern, which, upon subsequent exposure to an aqueous collagen solution, would allow protein deposition only on the hydrophilic regions. In this approach, it is of prime importance to develop a reliable and reproducible method of micropatterning collagen and to test the ability of hepatocytes to adhere to and function on this surface.

The objective of this study was to obtain selective adhesion of hepatocytes to a glass substrate with large regions of adhesive surface (AS) and nonadhesive surface (NAS) representing one stripe of a pattern. The AS had hydrophilic characteristics, whereas the NAS had hydrophobic characteristics, thereby mediating selective deposition of collagen molecules from an aqueous solution to the AS. Cell adhesion correlated with only the AS, suggesting selective collagen deposition onto the AS. Morphology and hepatocellular function on the AS was also shown to be similar to that observed in stable, differentiated sandwich cultures. Furthermore, mathematical modeling was used to approximate the operating constraints (*i.e.*, channel length and volume flow rate) of an ultimate micropatterned device in a large scale application.

MATERIAL AND METHODS

Surface Specifications

Three types of surfaces were used in this study: plain AS, plain NAS, and "banded" surfaces, as depicted in FIGURE 2. Disks of glass (5.08 cm diameter) with various surface coatings were obtained from Cytonix, Inc. (Beltsville, MD). AS were formed by spin-coating with urethane epoxy and curing in ultraviolet light. NAS were formed by overcoating with a solution of a fluorinated polymer. Banded

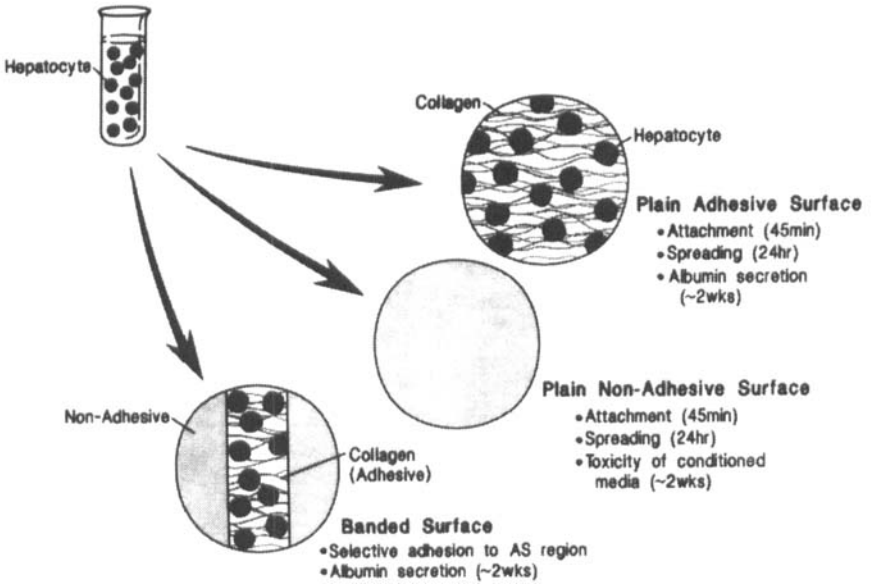

FIGURE 2. Schematic of experimental protocols used to obtain selective adhesion of hepatocytes. This study used both plain surfaces, entirely coated with a single polymer, and banded surfaces with a central band of AS flanked by NAS regions.

patterns were created by masking the urethane epoxy-coated surface with a single strip of adhesive tape of approximately 2 cm width. Disks were then overcoated with a fluorinated polymer (NAS) followed by removal of the tape, thereby exposing a band of adhesive surface (previously masked from overcoating) on a circular, otherwise nonadhesive surface.

Two banded surfaces with regions of AS and NAS were analyzed using atomic force microscopy (AFM) by Imaging Services (Santa Barbara, CA). Both disks were washed by agitation at 400 rpm (Model R-2 Linear Shaker, New Brunswick Scientific, Edison, NJ) for 1 min in distilled deionized water. One disk was imaged without any further treatment, whereas the other sample was spin-coated with 2 mL of 0.1 mg/mL collagen solution, as described below.

Preculture Processing of Surfaces

All surfaces were washed for 2 min in 3 mL of distilled, deionized water by shaking at 400 rpm on a shaker (New Brunswick Scientific). Surfaces were either plain AS or NAS or consisted of both types of coating on a single, banded surface, as shown in FIGURE 2. For attachment and spreading studies on plain surfaces, dilute collagen solutions (0.01% (w/v)) were prepared by mixing 1 part of 1.11 mg/mL collagen solution with 9 parts of distilled, deionized water. Solutions of 0.01% (w/v)

bovine serum albumin (BSA, Sigma, Lot Number 118F005) and 0.01% (w/v) poly-L-lysine (PL, Sigma) were prepared by dissolving directly in distilled, deionized water. Plain surfaces were coated with various solutions by immersing the surface into 300 mL of the appropriate solution at a 90° angle and a rate of 1 mm/s (for a total of 120 s per surface) using a modified Harvard syringe pump (Cambridge, MA) at 4°C.

On the other hand, for patterning studies, banded surfaces were spin-coated at 4°C. Spin-coating was used instead of immersion because it was found to produce better patterning results. Surfaces were clamped to the center of a modified centrifuge rotor using a machined accessory. A fixed volume of solution (2 mL of water or collagen type I solution) was pipetted onto the center of the surface for over 5 seconds. The solution was allowed to spread for 5 s prior to increasing the speed to 500 rpm for 20 s (including ramp time). The brake was applied for a duration of approximately 5 s until rotation had ceased. Although surfaces appeared dry immediately after spin-coating, they were also incubated at 37°C and 10% CO_2 for 30 min in 60 mm tissue culture dishes (Falcon) prior to cell seeding. Surfaces that were used for hepatocyte function studies were sterilized by treatment with ethylene oxide gas.

Isolation and Purification of Hepatocytes

Hepatocytes were isolated from 2- to 3-month-old adult female Lewis rats (Charles River, Boston, MA), weighing 180-200 g, by a modified procedure of Seglen.[19] Detailed procedures for isolation and purification of hepatocytes were previously described by Dunn *et al.*[13] Routinely, 200–300 million cells were isolated with viability between 85% and 95%, as judged by Trypan blue exclusion. Nonparenchymal cells, as judged by their size (less than 10 μm in diameter) and morphology (nonpolygonal or stellate), were less than one percent.

Attachment Assay and Morphological Measurements

Attachment and spreading studies were only performed with plain AS and NAS in order to show the selectivity of collagen-treated AS for hepatocytes. Two million freshly isolated, viable cells were seeded in 2 mL of medium on the appropriate pretreated surface (AS or NAS) or on a single layer of collagen gel (control) in a 60-mm tissue culture dish. Collagen isolation and purification from Lewis rat tail tendons is described in detail elsewhere.[13] AS and NAS were pretreated by immersion into a bath of collagen type I, BSA, PL, or water as described previously. Cells were spread evenly and incubated for 45 min at 37°C and 10% CO_2. After incubation, the cells were washed two times as follows. Unattached cells and medium were aspirated, and 3 mL of medium was added to each dish. Dishes were agitated at 200 rpm on a linear shaker for a total of 4 minutes. After 2 min, the orientation of the dishes was changed by rotating each dish 90° in the horizontal plane, and shaking was resumed for the remaining 2 minutes. Seeding efficiency on control collagen gels was ~90%. Finally, media were aspirated and 2 mL of media was added to each dish. Cells were recorded at 50 × magnification using a video system consisting of

an Olympus microscope (CK2, Japan), camera (Hamamatsu C-2400, Japan), monitor (Sony PVM1343MD, Japan), and VCR (Panasonic, AG-6750, Japan). The number of remaining cells in 10 random fields were counted from the recorded images using an image analysis system (Argus 10, Hamamatsu). Morphological measurements were made by recording the cells at 200 × magnification after 24 h of incubation at 37°C and 10% CO_2. The projected surface area (PSA) of the cells was analyzed from the recorded images using the image analysis system (Argus 10), which had been calibrated using a hemocytometer grating.

Hepatocyte Culture

Hepatocyte function obtained on the three types of surfaces (*i.e.*, plain AS, plain NAS, and banded pattern) used in this study were compared to that obtained in standard sandwich gel cultures. Collagen sandwich gels were prepared by first distributing 1 mL of type I collagen solution prepared from Lewis rat tail tendons.[13] The collagen solution was prepared by mixing 9 parts of 1.11 mg/mL collagen stock with 1 part of 10 × solution of Dulbecco's modified Eagle's medium (DMEM, Hazelton, Lenexa, KS). Collagen solution was chilled on ice, mixed just prior to use, spread evenly over a 60-mm tissue culture dish (Falcon, Lincoln Park, NJ), and allowed to gel at 37°C for 30 minutes. Two million viable hepatocytes in 2 mL of culture medium were seeded on this first collagen gel layer and allowed to attach for 24 h at 37°C and 10% CO_2. Because adult hepatocytes do not undergo significant cell division in sandwich culture, cell number can be assumed to be relatively constant over two weeks.[20] Culture medium was DMEM supplemented with fetal bovine serum, insulin, glucagon, epidermal growth factor, and hydrocortisone.[13] The culture medium was aspirated, and the cells were overlaid with a second layer (1 mL) of collagen gel solution. After 4 min at 37°C and 10% CO_2 to allow for gelation of the second collagen layer, 2 mL of culture medium was added. The medium was changed daily and stored at 4°C for secreted protein analysis.

Hepatocyte culture was also performed to assess toxicity of AS and NAS in the plain and banded configurations. Plain AS configuration were treated by immersion into a 0.5 mg/mL collagen solution. After 24 h, the hepatocytes were sandwiched by application of a standard collagen gel overlay. The toxic effects of NAS were investigated by incubation of standard sandwich cultures with medium conditioned with a plain NAS (3 mL of medium per NAS for 24 h at 37°C). This change in protocol was required because high-density cultures necessary for assessment of albumin secretion could not be obtained directly on NAS (because most hepatocytes did not attach). In the case of banded surfaces with selectively adhered hepatocytes, a layer of collagen gel was overlayed after 24 hours. Hepatocytes on the banded surface were seeded at 3 million per dish (to account for only 46% adhesive surface) and 2 million per dish in control cultures.

Albumin Secretion

Albumin secretion in all three cases was compared to that of a standard sandwich culture. Collected media samples were analyzed for secreted rat albumin content by

enzyme-linked immunosorbent assays (ELISA). Chromatographically purified albumin was purchased from Cappel (Cochranville, PA). The 96-well plates (NUNC-Immuno Plate, Maxisorp, Newbury Park, CA) were coated with 100 μL of rat albumin in 25 mM carbonate buffer, pH 9.6, overnight at 4°C. The wells were washed four times with PBS plus 0.5% (v/v) Tween 20 (PBS-Tween). Fifty microliters of sample were mixed with an equal volume of peroxidase, conjugated to rat albumin antibody (800 ng/mL in PBS-Tween). After overnight incubation at 4°C, the wells were washed four times with PBS-Tween and were developed with 100 μL of 25 mM citrate and 50 mM phosphate, pH 5, and 0.4 mg/mL *o*-phenylenediamine and 0.012% (v/v) hydrogen peroxide. The absorbance was measured at 490 nm with a Dynatech (Chantilly, VA) MR600 microplate reader. Concentrations of samples were determined from a standard curve generated for each ELISA plate.

Statistics and Data Analysis

Experiments were repeated two to three times. Each experimental condition included two to three dishes per data point. Two duplicate wells were averaged for each ELISA sample. One representative experiment is presented where the same trends were seen in multiple trials but absolute rates of secretion varied. Attachment data were quantified by dividing number of cells attached to a given surface by the number of cells attached to a single layer of collagen gel (control) and expressed as a percentage. Each data point represents the average of 10–20 fields. Morphological measurements were quantified by analyzing the PSA for 5 random cells in 10 random fields, per condition. Error bars represent standard deviation from the mean. Statistical significance was determined using the Student *t* test, assuming unequal variances.

Oxygen Distribution and Viscous Pressure Drop in Microchannels

Mathematical modeling of the oxygen distribution and the viscous pressure drop in a typical microchannel (FIG. 1) were used to predict characteristic dimension and the appropriate range of operating conditions for the ultimate design of a micropatterned device. Several assumptions were made in developing this model. First, the velocity profile was assumed to be fully developed, laminar plug flow traveling at the mean fluid velocity with negligible axial diffusion of oxygen. In addition, hepatocytes are modeled as a confluent array of cells that account for a constant oxygen uptake rate at the cell surface. Given these assumptions, the oxygen transport in the liquid flowing along the channel can be modeled as a combination of axial convection and radial diffusion. The dimensionless transport equation described in the oxygen distribution is as follows:

$$\frac{\partial \hat{c}}{\partial \hat{x}} = \frac{\partial^2 \hat{c}}{\partial \hat{y}^2}, \tag{1}$$

where $\hat{c}$ (= $[c - c_i]/c_i$) is the dimensionless oxygen concentration, such that the dimensionless inlet value is 0; $\hat{x}$ (= x/D_h Pe) is the dimensionless axial coordinate;

$\hat{y}$ (= y/D_h) is the dimensionless radial coordinate; D_h (= $4A/P$) is the hydraulic diameter; Pe (= $u_m D_h/D$) is the Peclet number; c and c_i are oxygen concentration and inlet oxygen concentration, respectively; P is channel perimeter; A is the cross-sectional channel area; and u_m is mean velocity of the fluid. The boundary conditions are

$$\frac{\partial c}{\partial \hat{y}} = 0 \qquad \text{at } \hat{y} = 0, \tag{2}$$

$$\hat{c} = 0 \qquad \text{at } \hat{x} = 0, \tag{3}$$

$$\frac{\partial \hat{c}}{\partial \hat{y}} = -\frac{V_m \rho D_h}{D c_i} = R \qquad \text{at } \hat{y} = \frac{L}{D_h}. \tag{4}$$

V_m is the maximal oxygen uptake rate, ρ is the cell density, and D is the diffusivity of oxygen in liquid. Equation 4 is a simplification of the Michaelis-Menten model of oxygen uptake rate, assuming that cells are consuming oxygen at the maximal rate.

The analytical solution of equations 1 and 4 is given as follows:[21]

$$\hat{c} = R\left[\left(\frac{\hat{x}}{L} + \frac{3\hat{y}^2 - L^2}{6L}\right) - \frac{2L}{\pi^2}\sum_{n=1}^{\sigma}\left(\frac{-1^n}{n^2} e^{-\frac{n^2\pi^2\hat{x}}{L^2}} \cos\frac{n\pi\hat{y}}{L}\right)\right]. \tag{5}$$

The partial pressure of oxygen can then be determined from the concentration and the solubility of oxygen in the liquid k, as follows: $P_{O_2} = c/k$. TABLE 1 summarizes the constants used in the solution of equation 5.

In order to predict the pressure drop along the microchannels, the one-dimensional Navier-Stokes approximation can be used to describe the momentum transport in the channels as follows:

$$\Delta P = \frac{12\,\mu Q L_c}{wh^3}, \tag{6}$$

where P is the hydrostatic pressure, μ is the viscosity of the fluid, Q is the volumetric flow rate, L_c is channel length, w is channel width, and h is channel height.

In rectangular duct flow, a velocity gradient exists in the y-direction as well as the larger gradient in the z-direction. This is the gradient responsible for shear forces

TABLE 1. Constants Used in the Solution of the Transport Equations

Symbol	Description	Value	Ref.
c_i	initial O_2 concentration	71.4 nmol/mL	
D	diffusivity of O_2 in liquid	2×10^{-5} cm^2/s	43
k	solubility of O_2 in liquid	1.19 nmol/mL/mm Hg	43
μ	viscosity of media at 37°C	0.007 g/cm/s	44
V_m	maximal oxygen uptake rate	0.36 nmol/s/10^6 cells	31

at the cell surface. Therefore, the shear stress, τ, on the cell surface is approximated as a function of the velocity gradient in the y-direction. A two-dimensional series approximation[22] of the velocity profile was used to calculate the shear stress at the midpoint of the cell surface as follows: $\tau = \mu(\partial u/\partial y)$ at $y = w/2$.

RESULTS

The development of a hepatocyte-based micropatterned device, using alternating AS and NAS, requires the ability to manipulate cell adhesion to a solid substrate. In our study, the potential for selective adhesion of hepatocytes was investigated using three different surfaces: plain AS, plain NAS, and banded patterns. Substrates were characterized for their ability to promote protein deposition using atomic force microscopy in the absence of cells. After cell seeding, surfaces were evaluated for their ability to support attachment, spreading, and differentiated function of hepatocytes. Finally, a mathematical model was used to determine the feasibility of the proposed micropatterned device and design parameters necessary for scaleup of the system.

Surface Characterization

The contact angles of AS and NAS with distilled water were visually estimated by adding 50 μL of water onto each surface at ambient temperature. The contact angles were approximately 50° and 100° for AS and NAS, respectively. In addition, banded surfaces were characterized before and after surface coating with aqueous collagen type I, using AFM. Spin-coating a banded surface with an aqueous collagen solution resulted in selective deposition of collagen onto the AS with no observable change in the NAS (FIG. 3). A layer of protein, presumed to be collagen type I, is visible on the AS region, whereas the NAS portion of the image displays striations of 10-100 nm in height.[23] In addition, other images taken at lower magnification show that the NAS-associated striations begin approximately 5 μm before the NAS interface begins, possibly indicating a resolution limitation to this processing technique (data not shown). Taken together, these results suggest that AS is more hydrophilic than NAS, and, thus, selective wetting of the AS by spin-coating with aqueous collagen solution resulted in selective collagen deposition on the AS and drying artifacts on the NAS.

Surface-hepatocyte Interaction in Plain AS and NAS Configuration

The hepatocyte-surface interaction was first assessed separately for both plain AS and plain NAS (FIG. 2). Surfaces were evaluated for the level of hepatocyte attachment, spreading, and differentiated function. The NAS tends to discourage wetting by an aqueous solution because of its hydrophobic properties. Conversely, the AS is wettable and thereby promotes adhesion of the water-based protein solution.

Attachment to various processed surfaces was expressed as a percent of the cells that attached to a similarly processed standard collagen gel. Cells were seeded on AS

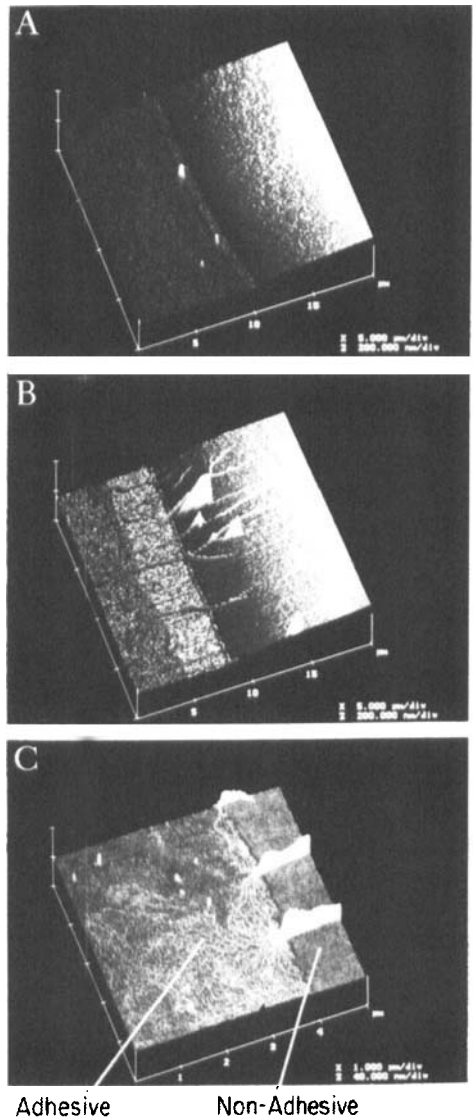

FIGURE 3. Atomic force microscopy image of the interface between AS (left) and NAS regions of a banded surface. Before spin-coating with aqueous collagen (**A**), after spin-coating with aqueous collagen (**B**), and higher magnification after spin-coating with aqueous collagen (**C**). A layer of protein is visible on the AS region, whereas the NAS portion of the image displays striations of 10–100 nm in height. Striations are a common drying artifact caused by uneven drying of the surface.[23]

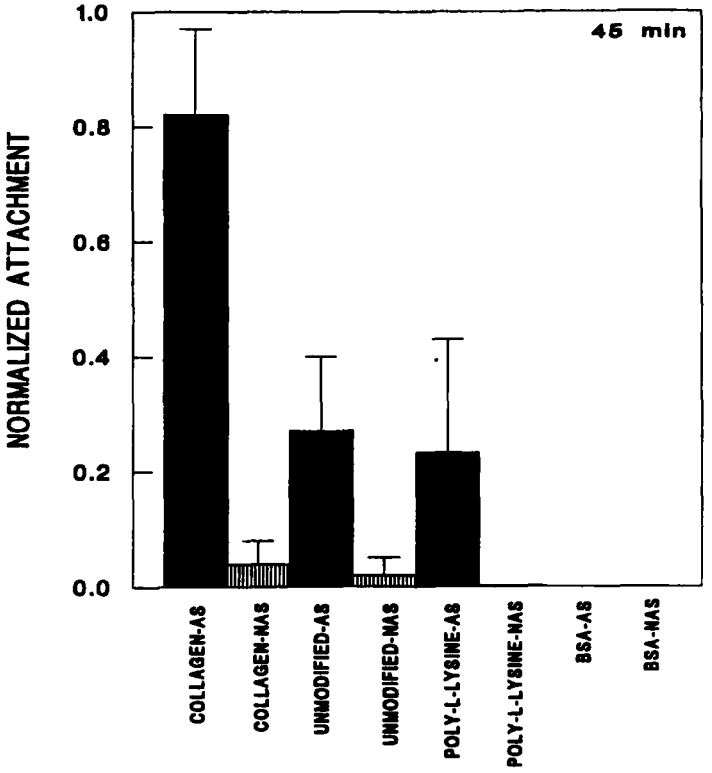

FIGURE 4. Attachment of hepatocytes to various pretreated substrates. Attachment was evaluated after a 45-min incubation period and expressed as a fraction of those remaining on a similarly treated single layer of collagen gel control. Plain AS and NAS were dipped at 1 mm/s in solutions containing 0.1 mg/mL of collagen type I (C), BSA, PL, or water (unmodified). $p < 0.001$ for collagen-AS versus collagen-NAS, collagen-AS versus unmodified-AS, and collagen gel control versus unmodified-AS. $p < 0.025$ for collagen gel control versus collagen-AS.

and NAS that had been treated by immersion in various solutions: collagen, PL, BSA, and water. BSA has a net negative charge at physiological pH, whereas PL carries a positive charge. These two molecules were used to attempt to distinguish nonspecific charge interactions from receptor-mediated attachment. FIGURE 4 compares adhesion of hepatocytes to a variety of pretreated surfaces. Collagen-treated AS showed the largest levels of attachment at 82.2 ± 15% of control. AS treated with a PL solution and water alone also displayed small levels of attachment (~25%), whereas attachment for all other conditions was less than 4% of control.

PSA was used to quantify the hepatocyte-substrate interaction at a later time point (24 h) following the early attachment phase. FIGURE 5 shows the average PSA of individual cells on various surfaces. Cultures on collagen-treated AS had a PSA of

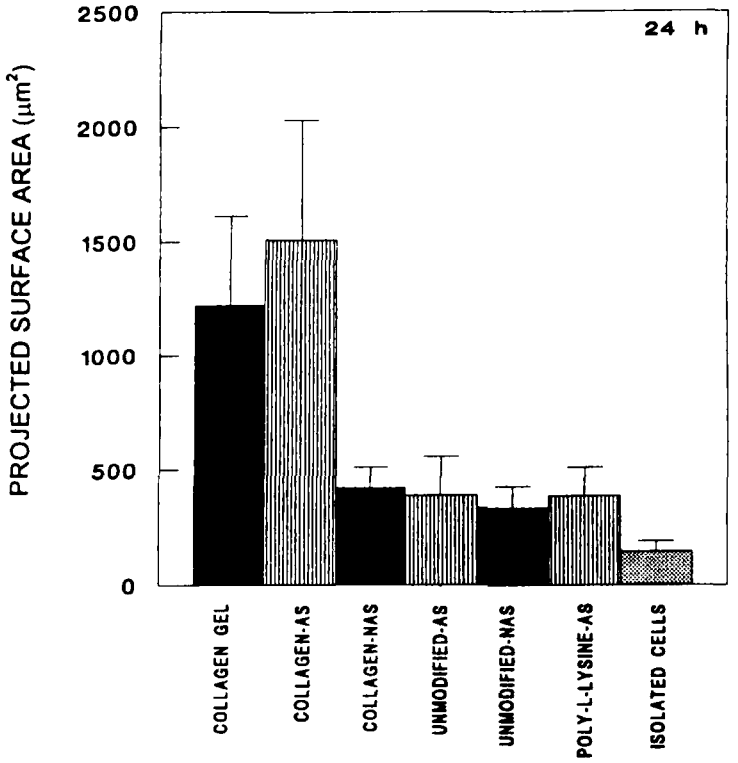

FIGURE 5. Projected surface area per cell of hepatocytes attached to pretreated substrates after 24 h. Cultures on collagen-treated AS had a PSA comparable to that of cells cultured on collagen gel controls. Nonbanded AS and NAS were dipped at 1 mm/s in solutions containing 0.1 mg/mL of collagen type I (C), BSA, PL, or water (unmodified). $p < 0.001$ for collagen-AS versus collagen-NAS, collagen-AS versus unmodified-AS, collagen-AS versus unmodified-NAS, collagen gel control versus unmodified-AS, and collagen gel control versus collagen-AS.

1508 ± 521 μm^2 and were comparable to the PSA of cells cultured on a conventional collagen gel (1221 ± 390 μm^2). Cells on all other surfaces remained round with a PSA of 300 to 500 μm^2. These results indicate that only the collagen-coated surfaces could provide the surface environment necessary for normal attachment and spreading.

To assess the potential toxic effects of AS and NAS on long-term hepatocellular function, sandwich cultures were performed under different surface conditions, and albumin secretion was measured. One representative experiment is shown; similar results were obtained three times. FIGURE 6 shows differentiated function of hepatocytes on AS with a collagen gel overlay as compared to standard sandwich culture. Both culture conditions produced increasing albumin secretion that reached

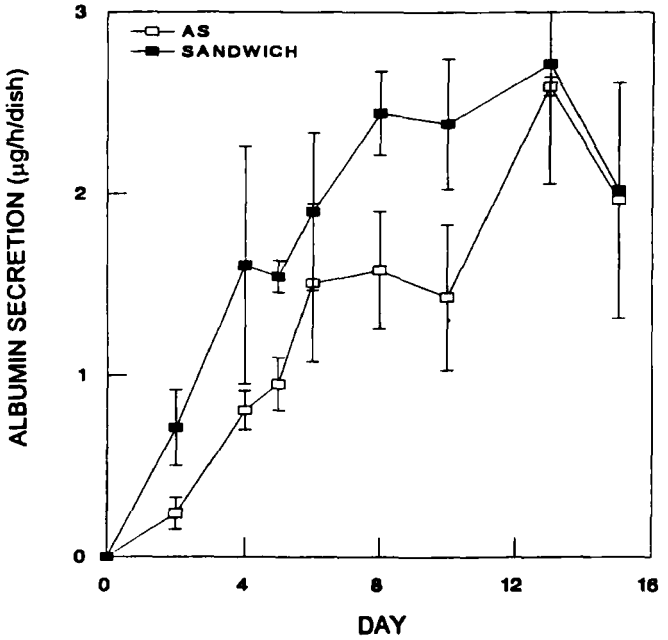

FIGURE 6. Toxicity of AS to albumin secretion of hepatocytes. Hepatocytes were seeded on AS and subsequently overlayed with collagen gel to mimic sandwich culture. Control cultures involved standard sandwich culture between two layers of collagen gel. A representative experiment is shown here, although the same qualitative results were obtained three times. n=4 for each individual experiment.

a plateau at approximately 2.5 µg/h/2 × 10^6 cells at approximately day 9. To determine the toxic effects of NAS, standard sandwich cultures were incubated with medium conditioned with an NAS. As mentioned earlier, cells could not be cultured directly on NAS because hepatocytes are anchorage-dependent cells. FIGURE 7 indicates comparable levels of albumin secretion for sandwich cultures incubated in standard media and media conditioned with NAS. Albumin secretion was similar for both conditions and reached a plateau level of 1.5 µg/h/2 × 10^6 cells at day 8. These results indicate that cells on AS have stable, long-term albumin secretion, and NAS is not toxic to hepatocytes.

Banded Surface-hepatocyte Interactions

The characterization of hepatocyte function on each plain surface was followed by studies where banded surfaces were used. The optimal concentration of the collagen solution used in spin-coating was investigated for patterning efficiency by varying the coating concentration between 2 mg/mL and 0.005 mg/mL. Coating concentrations that mediated both high levels of attachment on the AS and low levels

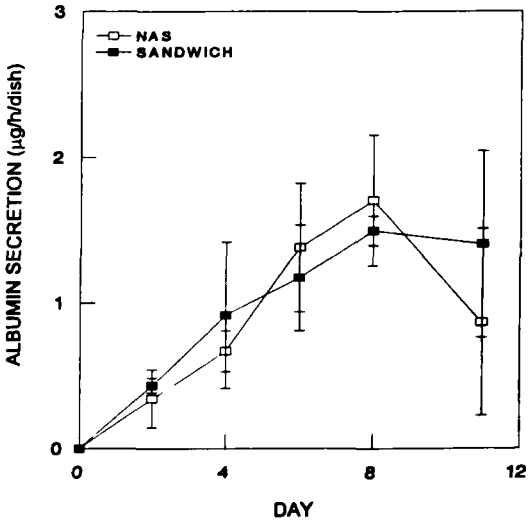

FIGURE 7. Toxicity of NAS to albumin secretion of hepatocytes. Hepatocytes in sandwich configuration were cultured with preconditioned media (with NAS) and compared to a standard sandwich control. A representative experiment is shown here, although the same qualitative trend was repeated three times. n = 4 for each individual experiment.

of attachment on the NAS satisfied the criteria for efficient patterning. An optimal range between 0.01 and 1 mg/mL was found (data not shown), and all subsequent experiments were performed with 0.1 mg/mL collagen solution. FIGURE 8 shows hepatocytes that have adhered to a banded surface that had been spin-coated with 0.1 mg/mL collagen solution after 24 h of culture. This is a typical field along the boundary of the two-surface coatings. The cells maintained their characteristic polygonal morphology and did not spread or migrate beyond the AS boundary during a 16-day culture period.

The persistence of differentiated function in the patterned hepatocytes was investigated using albumin secretion as a marker. A layer of gel was applied over the selectively adhered hepatocytes at day one to mimic the standard sandwich culture configurations. FIGURE 9 shows a steady increase of albumin secretion until a plateau was reached at day 12 at ~2.2 μg/h/dish. This behavior was similar to that of the standard sandwich control.

In summary, we have investigated protein deposition, cell adhesion and spreading, and albumin secretion in plain AS, plain NAS, and banded configurations. Studies on banded surfaces with regions of AS and NAS showed collagen deposition primarily on AS. Collagen-treated plain AS was subsequently found to preferentially support significant levels of attachment and spreading of cells as compared to negligible attachment and spreading on plain NAS. Finally, banded patterns were found to support selective adhesion of hepatocytes and stable albumin secretion on the AS region of the pattern.

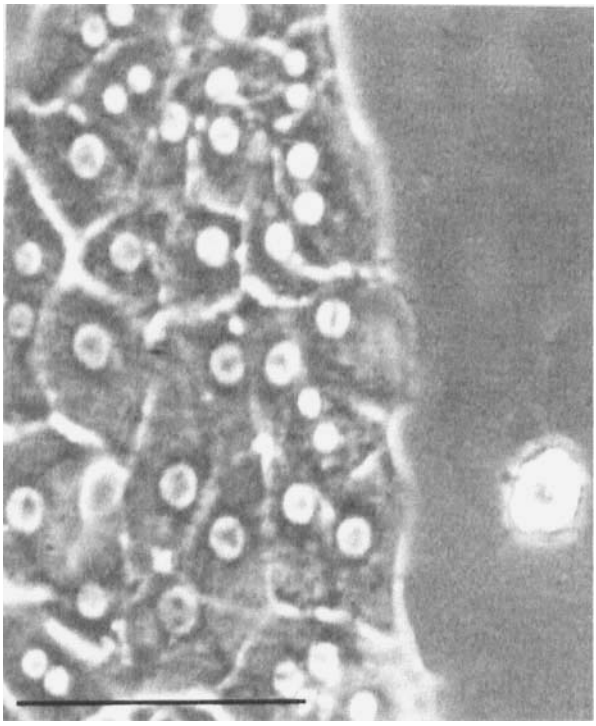

FIGURE 8. Micrograph of selective adhesion of hepatocytes to a banded surface. This banded surface was spin-coated with 2 mL of 0.1 mg/mL collagen solution. Scale bar corresponds to 100 μm.

Model Predictions

Given our success in maintaining functional hepatocytes on patterned surfaces, we chose to investigate theoretically important design requirements necessary for scaleup of a micropatterned device. Mathematical modeling of the oxygen distribution and the viscous pressure drop in a typical microchannel of an idealized micropatterned device was used to predict characteristic dimensions and the appropriate range of operating conditions for ultimate bioreactor design. The maximum allowable channel length with no oxygen limitations to hepatocytes (*i.e.*, critical length) was calculated using an oxygen distribution model. In this calculation, the inlet partial pressure was defined as 60 mm Hg,[24] and the lower limit of acceptable oxygen partial pressure was defined as 5 mm Hg ($10 \times K_m$). The channel length where this partial pressure was achieved was mathematically defined as the critical channel length, L_c. As expected, increasing flow rates (proportional to Pe) resulted in proportional increases in critical channel length (FIG. 10). Furthermore, the influence of channel geometry on critical channel length was also investigated, and the L_c was found to be fairly insensitive to changes in height and width of the channel (*i.e.*, less than 7.5% for 50% reduction in width, data not shown).

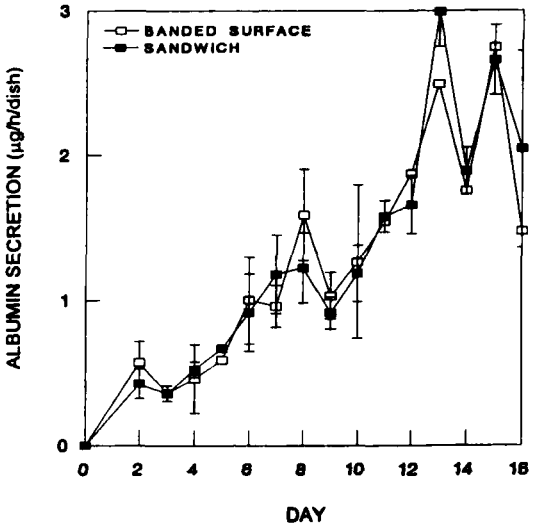

FIGURE 9. Albumin secretion of hepatocytes on a banded surface. Banded surfaces with selectively adhered hepatocytes were overlayed with a layer of collagen gel and compared to sandwich cultures between two layers of collagen gel. A representative experiment is shown here, although the same qualitative trend was repeated twice. n=4 for each individual experiment.

In order to characterize the limitation imposed on the micropatterned device by the pressure drop across the channels, typical *in vivo* values were used as an upper limit. Hydrostatic pressure has been measured *in vivo* between 9.5 and 1.5 mm Hg from the portal vein to the hepatic vein.[25] By limiting the viscous pressure drop to 8 mm Hg, a relationship between the flow rate and the critical length was generated. Combining the opposing limitations of viscous pressure drop and oxygen concentration on the critical channel length and low rate resulted in a somewhat limited operating regime (FIG. 10). The longest achievable channel length taking oxygen and pressure drop limitations into account was approximately 0.6 cm, with an accompanying flow rate of approximately 2.0×10^{-6} mL/s in a 100 µm × 10 µm (width × height) channel. Shear stress in a typical microchannel for this flow rate was estimated at the cell surface and found to be in the range of 5–10 dynes/cm^2.

DISCUSSION

Two crucial criteria for the successful development of bioartificial liver devices are long-term stable hepatospecific function, and efficient mass transport to a large number of cells in a small volume. Micropatterning technology may be useful in satisfying both of these criteria. A key element in the development of a micropatterned, bioartificial liver device is the ability to selectively deposit hepatocytes on certain solid substrates while keeping other surfaces cell free. In this study, we demonstrated that, in principle, we can reproducibly attach hepatocytes to patterned

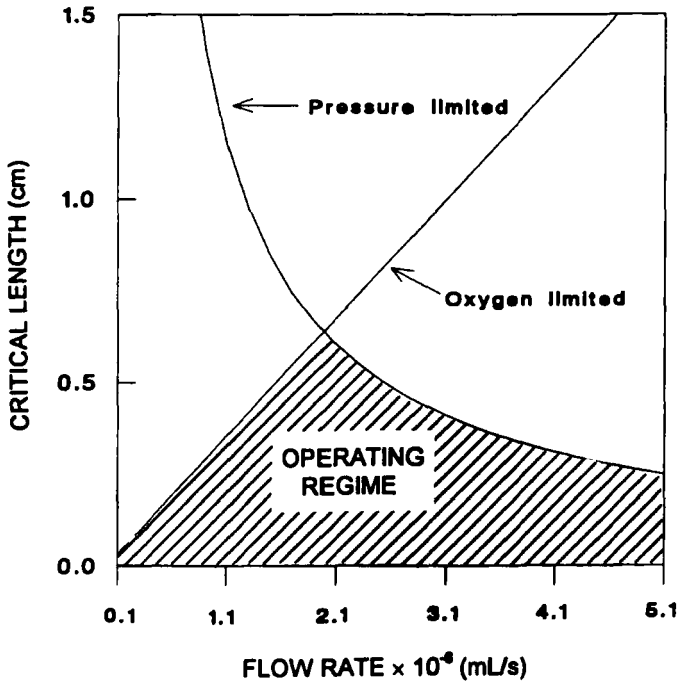

FIGURE 10. Maximum microchannel path length dictated by a model of oxygen distribution and viscous pressure drop. The line labeled "oxygen limited" refers to maximum microchannel path length to maintain all cells at 5 mm Hg O_2 or greater. The line labeled "pressure limited" refers to the maximal channel length to maintain the viscous pressure drop to 8 mm Hg or less.

substrates. The selective adhesion attained in our study was achieved by exposing the AS and NAS to an aqueous collagen type I solution, resulting in preferential wetting of the AS due to its relatively hydrophilic nature as compared to NAS. Given the selective deposition of protein (collagen) molecules on the AS, efficient cell adhesion occurred solely on the AS. In addition to adhesion, hepatocytes displayed normal morphology and differentiated function in long-term culture.

AFM characterization of banded surfaces showed deposition of a layer of protein only on the AS regions of the banded surface. This result suggests that the selective wetting of the hydrophilic AS region with aqueous collagen solution resulted in the deposition of collagen onto AS only. Further indirect evidence that collagen was deposited onto the AS only came from our attachment studies with hepatocytes discussed below. Moreover, direct surface examination by AFM revealed striation patterns on the NAS regime. Striations are a common artifact caused by uneven drying of the surface.[23] This distribution of striations can be expected if the NAS surface dewets more quickly than the AS, due to its relative hydrophobicity; the NAS subsequently underwent uneven drying. The dimensions (10-100 nm) of these striations correlated well with those reported in the literature for spin-coating.[23] Limita-

tions of this processing technique stem from the boundaries on resolution that may occur at smaller patterning widths. According to the AFM images, this limit is on the order of 5 μm, which corresponds to the distance from the interface at which NAS striations were observed. A number of independent variables exist for optimization: spinning speed, solution volume, spinning time, and temperature. These parameters were held constant for this preliminary study, although at smaller patterning widths, they may have a strong influence on the limit of resolution.

Hepatocytes, as anchorage-dependent cells, must attach and spread to function. In this study, a receptor-specific adhesion molecule, namely, collagen type I, was used to promote attachment. Both collagen type I and laminin have been shown to bind to a common integrin, $\alpha_2\beta_1$.[26] A spin-coating process was used to apply the collagen type I to AS regions of banded surfaces. Theoretically, the presence of collagen on the surface could be due to (1) selective wetting of AS and subsequent drying of the collagen solution, resulting in local collagen deposition or (2) energetically favorable collagen adsorption to the AS from a collagen solution. The entire coating process took about 30 seconds. Prior studies on the kinetics of collagen adsorption have shown on the order of 30 min to 1 h for half maximal levels of adsorption to occur.[27] Therefore, it is likely that no significant interactions between AS, NAS, and the collagen solution took place in the 30 s time frame, and thus deposition as opposed to adsorption was the dominant mechanism of collagen coating of AS. It is noteworthy to mention that in our earlier studies we have used dipping (versus spin-coating) to coat the AS region of banded surfaces with collagen. The dipping experiments occasionally produced collagen adsorption during the immersion procedure (120 s) to the hydrophobic, NAS, surface, which later became obvious due to nonspecific cell adhesion. Collagen adsorption may account for the inconsistency of patterning obtained by dipping (versus spin-coating) banded surfaces. Thus, spin-coating proved to be a more robust processing technique for selective coating of collagen onto the AS region of banded surfaces.

After spin-coating, cells were seeded on the substrates in media containing 10% serum. Serum contains adhesive proteins, such as fibronectin, which are known to adsorb to substrata and mediate cellular interactions.[28] In our system, cells were allowed to attach for 45 min prior to washing. In this time frame, it is conceivable that serum proteins could have adsorbed to and contaminated the NAS, thereby mediating nonselective attachment; however, hepatocytes on the NAS portion of the banded surfaces were readily removed during the rigorous washing protocol at the end of the 45-min attachment period. Therefore, we were able to reproducibly obtain selective adhesion of hepatocytes onto the AS portion of the banded surfaces in the presence of serum.

In choosing surfaces to promote attachment, two broad classes can be considered: (1) those that mediate their effects through nonspecific physicochemical interactions (*i.e.*, charge), and (2) those that mediate their effects through specific biological interactions. In our studies, collagen proved to be best at ensuring high levels of attachment. The unmodified AS and AS coated with PL also displayed some levels of attachment. The low rates of attachment seen on unmodified AS as compared to collagen-treated AS might be explained alternatively by (1) serum proteins that may adsorb during the 45-min cell incubation cause the unmodified AS to display low levels of attachment, or (2) the unmodified AS is slightly toxic, and thus fewer cells

attach during the 45-min cell incubation. Although we studied the toxic effects of collagen-coated AS over a two-week duration and did not find evidence of toxicity, we cannot entirely rule out the potential toxic effects of the uncoated AS. The attachment on the PL may have been due to either (1) lack of deposition of PL onto the surface, resulting in behavior of the surface like the unmodified AS, or (2) PL deposition mediating comparatively low, but significant, levels of attachment. We did not directly assay for the presence of PL on the surface; therefore, it is impossible to specify one of the two phenomena.

In general, cells seeded on collagen-coated AS spread significantly more than cells on other surfaces and displayed the characteristic polygonal morphology. Our PSA values, shown in FIGURE 5, can be compared to other studies based on an estimation of coating concentration. Spin-coating of a 0.1 mg/mL collagen type I solution of approximately viscosity, 0.008 centipoise, at 500 rpm for 25 s should yield a film of less than 3.5 μm thickness.[23] Given that the AS is approximately 46% of a 5.08 cm diameter disk, this corresponds to an upper estimate of a coating concentration of 35 ng/cm^2. Rubin *et al.*[29] correlated added collagen α_1(I) chains to bound chains in this regime and found approximately 40% of the protein bound to a tissue culture dish. This corresponds to an estimated bound protein concentration on the order of less than 14 ng/cm^2. Mooney *et al.*[30] reported a PSA of approximately 1500 μm^2 for a coating concentration of 1 ng/cm^2. This PSA correlates reasonably well with our PSA measurements on AS given that the estimated coating concentrations are within one order of magnitude of that reported by Mooney *et al.*[30] Furthermore, studies on PSA in sandwich cultures and on dried collagen coatings (1 ng/cm^2) have shown that a PSA of approximately 1500 μm^2 occurs when fully developed protein production and secretion occurs in hepatocytes.[30,31] Thus, hepatocytes on the collagen-coated AS, which spread to approximately 1500 μm^2, are more likely to display sustained differentiated function than hepatocytes on any of the other coatings used in this study where they displayed PSAs of less than 500 μm^2.

The mathematical modeling conducted in this study focused on obtaining a set of operating constraints for the hypothetical micropatterned device (FIG. 10). An assembly of typical microchannels would form a single plate in a multiplate extracorporeal liver support device. A number of assumptions were made in order to model the mass transfer and fluid mechanics of this system. Oxygen uptake rate was assumed to be constant and to occur at the maximal level (V_m) in equation 4. In our microchannel system, where oxygen delivery should be maintained above the K_m of the cells to prevent hypoxia and necrosis, the oxygen limitations on the uptake kinetics can be neglected. Furthermore, the oxygen uptake rate model at the cell surface neglected any intracellular oxygen gradients. In addition, our problem formulation assumed confluent hepatocytes, resulting in smooth channel walls. In the proposed micropatterned device, the channel wall would actually be composed of a series of spread cells with different geometries and potential regions of reduced flow and transport. Our interest in the lower, bound-on acceptable channel lengths, corresponding to the largest possible oxygen uptake in a microchannel device, is the justification for the overestimation of oxygen uptake rate. The oxygen distribution model also neglected axial diffusion, which is reasonable for large Pe, and the velocity profile was approximated as plug flow using the value of mean velocity to allow for the use of an analytical solution. Finally, the pressure drop in a channel was

approximated by equation 6 because more precise two-dimensional series approximations yielded minimal increased accuracy.[22]

Comparisons between the channel flow rate and length, and the *in vivo* sinusoidal volume flow rate and sinusoidal length can be made. The motivation for using the viscous pressure drop across a channel as an operating constraint on these parameters is the existence of a hydrostatic pressure drop (*i.e.*, blood pressure) *in vivo*. Possible effects of elevated hepatic vein pressures on liver function and structure have been explored in whole organ experiments, showing increased perisinusoidal space of Disse, decreased transport from blood due to increased vascular space, and irreversibly decreased bile secretion pressure.[32] In our microchannel model, hydrostatic pressure drop was, at first, limited to physiological levels (8 mm Hg). After building the device, one can experimentally investigate whether this constraint can be relaxed. The optimal channel length determined, using both the pressure and oxygen constraints, was 0.6 cm. This channel length can be compared to the *in vivo* length of the rat sinusoid of approximately 0.04 cm.[33] Similarly, for *in vivo* sinusoidal cross-sections of the same order as the cross-sections used in our calculations, volumetric flow rates have been measured to be approximately 0.1×10^{-6} mL/s as compared to microchannel flow rates of 2.0×10^{-6} mL/s.[34] It is noteworthy that both channel length and volumetric flow rate in the device are within one order of magnitude of *in vivo* values.

The estimated channel length and flow rates can also be used to assess the feasibility of scaleup of a microchannel device. Asonuma *et al.*[35] determined that as little as 12% (by weight) of the rat liver is sufficient for liver support of the animal. Therefore, assuming a cell diameter of approximately 40 μm, channel length of 0.6 cm, channel width of 100 μm, AS width of 50 μm, and the necessity of 60 million cells per device (approximately 10% of the parenchymal cells in a 200 g rat), a value of 400,000 channels per device is obtained. If one assumes each plate of the eventual device to be 20 cm wide, this would translate to 300 plates per device. Furthermore, if one assumes the glass plates to be approximately 0.5 mm thick, this would correspond to a device of approximately 15 cm in height. The dead volume[f] associated with such a device for use in a rat would be 2.4 mL with a device flow rate of 0.8 mL/s and a shear stress of 5–10 dynes/cm^2. These values seem reasonable as compared to the total blood volume (10–13 mL) and cardiac output (0.25–1.33 mL/s) of a rat[36] and reported deleterious shear stresses for other mammalian cell types (in the range of 140 dynes/cm^2 for fibroblasts and >>24 dynes/cm^2 for endothelial cells).[37,38]

Conventional approaches to bioartificial liver devices include hollow fibers, cultured monolayers, and microcarriers. Hollow fibers with intraluminal cell seeding have been shown to suffer from necrosis, which was suggested to be due to mass transport limitations.[3] Focal necrosis has also been seen in extraluminal cell-seeding configurations.[39] Micropatterning could potentially address such mass transport limitations by allowing the manipulation of a diffusion path length through the channel width. In addition, monolayer cultures have been shown to function for a number of

[f]Dead volume is the fluid volume associated with a rat liver support device (excluding the volume of inlet and outlet lines), assuming a 100 μm × 10 μm (width × height) channel, a 50 μm (width) adhesive surface, and a hepatocyte diameter of 40 μm.

days with a dead volume of approximately 200 mL for 500×10^6 cells.[2] In comparison, theoretical calculations show that the same number of cells could potentially be maintained in a micropatterned configuration with a dead volume of approximately 25 milliliters. Finally, microcarriers, like micropatterning, offer an approach to obtain large cell densities in a relatively small volume. The flow rates necessary to supply oxygen and nutrients to this cell culture have the potential to produce large shear stresses due to the small voids (estimated $<<50\mu m$) between spheres.[40,g] By contrast, micropatterning may have controllable channel lengths, thereby limiting the flow rate necessary to supply nutrients to the distal cells, and controllable channel widths (of the order of 100 μm), thereby limiting the shear stresses on the cell surface.

SUMMARY

Successful development of cell-biased bioartificial liver devices necessitates the establishment of techniques and designs for long-term, stable hepatocellular function and efficient transport of nutrients and wastes within the device. Given the relatively large cell mass that one must consider, one possible solution involves the use of micropatterning technology to sandwich hepatocytes aligned in rows between two micropatterned surfaces. Rows of cells would alternate with hepatocyte-free areas, creating efficient transport channels for fluid flow and nutrient exchange. Ultimately, this type of device could also be used as a three-dimensional construct for investigating a variety of cell-surface, cell-extracellular matrix, and cell-cell interactions. To achieve this goal, one must develop techniques for selectively adhering hepatocytes to solid substrates. In this study, reproducible, selective adhesion of hepatocytes on a glass substrate with large regions of adhesive (AS) and nonadhesive (NAS) surfaces was obtained. The AS had hydrophilic characteristics, enhancing deposition of collagen molecules from an aqueous solution, and subsequent hepatocyte adhesion, whereas the NAS had hydrophobic properties and remained collagen-free and hepatocyte-free. In addition, a reproducible processing technique for obtaining patterns of hepatocytes was developed and optimized, using a surface with a single AS band as a first approximation to a micropatterned device. This was achieved by spin-coating an aqueous collagen type I solution (0.1 mg/mL) on a banded surface at 500 rpm for 25 seconds. The morphology and long-term function of the hepatocytes attached to AS in nonbanded and banded surface configurations was assessed by mimicking sandwich culture and was shown to be similar to stable, differentiated sandwich cultures. Mathematical modeling was used to determine critical design criteria for the hypothetical micropatterned device. The oxygen distribution and viscous pressure drop were modeled along a typical microchannel and limited to *in vivo* values. An optimal channel length of 0.6 cm and a flow rate of 2.0×10^{-6} mL/s were obtained for a channel of 100 μm in width and 10 μm in height. These values were reasonable in terms of practical implementation.

[g]This assumes a microcarrier diameter of 200 μm,[41] 100% confluency, and perfect bead packing.[42] Fifty micrometers is the typical path length of diffusion for a molecule being transported between the liquid phase and cell surface.

ACKNOWLEDGMENTS

Many thanks go to Drs. Jim Brown of Cytonix, Inc. and François Berthiaume, Brent Foy, and Howard Matthews of Massachusetts General Hospital.

REFERENCES

1. Takahashi, M., H. Matsue, M. Matsushita, K. Sato, M. Nishikawa, M. Koike, H. Noto, Y. Nakajima, J. Uchino, T. Komai & E. Hashimura. 1992. Does a porcine hepatocyte hybrid artificial liver prolong the survival time of anhepatic rabbits? ASAIO J. **38:** M468–M472.
2. Uchino, J., T. Tsuburaya, F. Kumagai, T. Hase, T. Hamada, T. Komai, A. Funatsu, E. Hashimura, K. Nakamura & T. Kon. 1988. A hybrid bioartificial liver composed of multiplated hepatocyte monolayers. ASAIO Trans. **34:** 972–977.
3. Nyberg, S. L., R. A. Shatford, M. V. Peshwa, J. G. White, F. B. Cerra & W. Hu. 1993. Evaluation of a hepatocyte-entrapment hollow fiber bioreactor: A potential bioartificial liver. Biotechnol. Bioeng. **41:** 194–203.
4. Sussman, N. L., M. G. Chong, T. Koussayer, D. He, T. A. Shang, H. H. Whisennand & J. H. Kelly. 1992. Reversal of fulminant hepatic failure using an extracorporeal liver assist device. Hepatology **16:** 60–65.
5. Shatford, R. A., S. L. Nyberg, S. J. Meier, J. G. White, W. D. Payne, W. Hu & F. B. Cerra. 1992. Hepatocyte function in a hollow fiber bioreactor: A potential bioartificial liver. J. Surg. Res. **53:** 549–557.
6. Jauregui, H. O., S. Naik, J. L. Driscoll, B. A. Solomon & P. M. Galletti. 1984. Adult rat hepatocyte cultures as the cellular component of an artificial hybrid liver. *In* Biomaterials in Artificial Organs. J. P. Paul, J. D. S. Gaylor, J. M. Courtney & T. Gilchrest, Eds. Macmillan Press. London, England.
7. Kasai, S., I. Oikaw, H. Asakawa, T. Yamamoto, M. Sawa, H. Sakata, K. Kondoh, T. Munakata, M. Mito & H. Tanzawa. 1984. Evaluation of an artificial liver support device using isolated hepatocytes. *In* Progress in Artificial Organs. K. Atsumi, M. Maekawa & K. Ota, Eds. **2:** 734–738. ISAO Press No. 204. Cleveland, OH.
8. Hager, J. C., R. Carman, L. E. Porter, R. Stoller, E. H. Leduc, P. M. Galletti & P. Calabresi. 1983. Neonatal hepatocyte culture on artificial capillaries: A model for drug metabolism and the artificial liver. ASAIO J. **6:** 26–35.
9. Shnyra, A., A. Bocharov, N. Bochkova & V. Spirov. 1991. Bioartificial liver using hepatocytes on biosilon microcarriers: Treatment of chemically induced acute hepatic failure in rats. Artif. Organs (Clevel.) **15:** 189–197.
10. Demetriou, A. A., N. M. Chowdury, S. Michalski, J. Whiting, R. Schechner, D. Feldman, S. M. Levenson & J. R. Chowdury. 1986. New method of hepatocyte transplantation and extracorporeal liver support. Ann. Surg. **204:** 259–270.
11. Rozga, J., F. Williams, M. Ro, D. Neuzil, T. D. Giorgio, G. Backäsch, A. D. Moscioni, R. Hakim & A. A. Demetriou. 1993. Development of a bioartificial liver: Properties and function of a hollow-fiber module inoculated with liver cells. Hepatology **17:** 258–265.
12. Arnaout, W. S., A. D. Moscioni, R. L. Barbour & A. A. Demetriou. 1990. Development of a bioartificial liver: Bilirubin conjugation in Gunn rats. J. Surg. Res. **48:** 379–382.
13. Dunn, J. C. Y., R. G. Tompkins & M. L. Yarmush. 1991. Long-term *in vitro* function of adult hepatocytes in a collagen sandwich configuration. Biotechnol. Prog. **7:** 237–245.
14. Ezzell, R. M., M. Toner, K. Hendricks, J. C. Y. Dunn, R. G. Tompkins & M. L. Yarmush. 1993. Effect of collagen gel configuration on the cytoskeleton in cultured rat hepatocytes. Exp. Cell Res. **208:** 442–452.
15. Britland, S., E. Perez-Arnaud, P. Clark, B. McGinn, P. Connolly & G. Moores. 1992. Micropatterning proteins and synthetic peptides on solid supports: A novel application for microelectronics fabrication technology. Biotechnol. Prog. **8:** 155–160.
16. Stenger, D. A., J. H. Georger, C. S. Dulcey, J. J. Hickman, A. S. Rudolph, T. B. Nielsen, S. M. McCort & J. M. Calvert. 1992. Coplanar molecular assemblies of amino and

perfluorinated alkylsilanes: Characterization and geometric definition of mammalian cell adhesion and growth. J. Am. Chem. Soc. **114:** 8435–8442.
17. MATSUDA, T., T. SUGAWARA & K. INOUE. 1992. Two-dimensional cell manipulation technology. ASAIO J. **38:** M243–M247.
18. BISSELL, D. M. 1981. Primary hepatocyte culture: Substratum requirements and production of matrix components. FASEB J. **40:** 2469–2473.
19. SEGLEN, P. O. 1976. Preparation of isolated rat liver cells. Methods Biol. **13:** 29–83.
20. DUNN, J. C. Y., M. L. YARMUSH, H. G. KOEBE & R. G. TOMPKINS. 1989. Hepatocyte function and extracellular matrix geometry: Long-term culture in a sandwich configuration. FASEB J. **3:** 174–177.
21. CARSLAW, H. S. & J. C. JAEGER. 1959. Conduction of heat in solids. Oxford. Oxford, England.
22. WHITE, F. 1974. Viscous Fluid Flow. McGraw-Hill. New York.
23. ELLIOTT, D. J. 1989. Integrated Circuit Fabrication Technology. McGraw-Hill. New York.
24. DE GROOT, H., A. LITTAUER & T. NOLL. 1988. Metabolic and Pathological Aspects of Hypoxia in Liver Cells. *In* Oxygen Sensing in Tissues. H. Acker, Ed. Springer-Verlag.
25. NAKATA, K., G. F. LEONG & R. W. BRAUER. 1960. Direct measurement of blood pressures in minute vessels of the liver. Am. J. Physiol. **6:** 1181–1188.
26. STATZ, W. D., K. F. FOK, M. M. ZUTTER, S. P. ADAMS, B. A. RODRIGUEZ & S. A. SANTORO. 1991. Identification of a tetrapeptide recognition sequence for the alpha-2 beta-1 integrin in collagen. J. Biol. Chem. **266:** 7363–7367.
27. DEYME, M., A. BASZKIN, J. E. PROUST, E. PEREZ & M. M. BOISSONNADE. 1986. Collagen at Interfaces I. *In situ* collagen adsorption at solution/air and solution/polymer interfaces. J. Biomed. Mater. Res. **20:** 951–962.
28. HORBETT, T. A. 1982. Protein adsorption on biomaterials. *In* Biomaterials: Interfacial Phenomena and Applications. S. L. Cooper & N. A. Peppas, Eds. American Chemical Society, Washington, D.C.
29. RUBIN, K. & M. HOOK. 1981. Substrate adhesion of rat hepatocytes: Mechanism of attachment to collagen substrates. Cell **24:** 463–470.
30. MOONEY, D., L. HANSEN, J. VACANTI, R. LANGER, S. FARMER & D. INGBER. 1992. Switching from differentiation to growth in hepatocytes: Control by extracellular matrix. J. Cell. Physiol. **151:** 497–505.
31. ROTEM, A., M. TONER, R. G. TOMPKINS & M. L. YARMUSH. 1992. Oxygen uptake rates in cultured hepatocytes. Biotechnol. Bioeng. **40:** 1286–1291.
32. BRAUER, R. W., R. J. HOLLOWAY & G. F. LEONG. 1959. Changes in liver function and structure due to experimental passive congestion under controlled hepatic vein pressures. Am. J. Physiol. **197:** 681–692.
33. YAMAMOTO, K., I. SHERMAN, M. J. PHILLIPS & M. M. FISHER. 1985. Three-dimensional observations of the hepatic arterial terminations in rat, hamster and human liver by scanning electron microscopy of microvascular casts. Hepatology **5:** 452–456.
34. KOO, A., I. Y. S. LIANG & K. K. CHENG. 1975. The terminal hepatic microcirculation in the rat. Q. J. Exp. Physiol. **60:** 261–266.
35. ASONUMA, K., J. C. GILBERT, J. E. STEIN, T. TAKEDA & J. P. VACANTI. 1992. Quantitation of transplanted hepatic mass necessary to cure the Gunn rat model of hyperbilirubinemia. J. Pediatr. Surg. **27:** 298–301.
36. VAN DONGEN, J. J., R. REMIE, J. W. RENSEMA & G. H. J. VAN WUNNIK. 1990. Manual of Microsurgery on the Laboratory Rat. J. P. Huston, Ed. Elsevier. Amsterdam.
37. TRUSKEY, G. A. & J. S. PIRONE. 1990. The Effect of Fluid Shear Stress Upon Cell Adhesion to Fibronectin-treated Surfaces. J. Biomed. Mater. Res. **24:** 1333–1353.
38. FRANGOS, J. A., L. V. MCINTIRE & S. G. ESKIN. 1988. Shear stress induced stimulation of mammalian cell metabolism. Biotechnol. Bioeng. **32:** 1053–1060.
39. WOLF, C. F. W. & B. E. MUNKELT. 1975. Bilirubin conjugation by an artificial liver composed of cultured cells and synthetic capillaries. Trans. ASAIO **21:** 16–27.
40. BERTHIAUME, F., M. TONER, R. G. TOMPKINS & M. L. YARMUSH. 1993. Implantation biology: the Response of the Host. *In* Tissue Engineering in Implantation Biology. R. S. Greco, Ed. 363–386. CRC Press. Boca Raton, FL.
41. FOY, B. D., J. LEE, J. MORGAN, M. TONER, R. G. TOMPKINS & M. L. YARMUSH. 1993.

Optimization of hepatocyte attachment to microcarriers: Importance of oxygen. Biotechnol. Bioeng. **42:** 579–588.

42. COULSON, J. M., J. F. RICHARDSON, J. R. BACKHURST & J. H. HARKER. 1980. Chemical Engineering VII: Unit Operations. Pergamon Press. Oxford.
43. YARMUSH, M. L., M. TONER, J. C. Y. DUNN, A. ROTEM, A. HUBEL & R. G. TOMPKINS. 1992. Hepatic tissue engineering: Development of critical technologies. Ann. N.Y. Acad. Sci. **665:** 238–252.
44. VAN KOOTEN, T. G., J. M. SCHAKENRAAD, H. C. VAN DER MEI & H. J. BUSSCHER. 1992. Development and use of a parallel-plate flow chamber for studying cellular adhesion to solid surfaces. J. Biomed. Mater. Res. **26:** 725–738.